Master of Science Thesis

Developing and evaluating strategies to deal with motion induced artefacts in functional magnetic resonance imaging

Mikael Petersson

Supervisor: Anthony Brian Waites,

The work has been performed at
Brain Research Institute,
Melbourne, Victoria, Australia

Medical Radiation Physics
Clinical Sciences, Lund
Lund University, 2006

1. Introduction

Functional magnetic resonance imaging (fMRI) is a non-invasive way to map human brain activation. The method can be used to gather pre-surgical information before removal of pathological tissue or to map functional areas of the brain. One can compare the distribution of functional areas between volunteers and a patient group with certain disease or disorder to identify a pathological difference between the two groups.

The accuracy of the examination is greatly dependent on the subject's ability to stay still inside the MR scanner. Patient movement can induce effects that corrupt image data that can lead to fMRI examination failure. Subject motion is one of the most common causes of examination failure [1].

The fMRI time series is generated by letting a patient in the MR scanner change between two different cognitive states, e.g. rest/task during the scan, e.g. collecting a set of image volumes when subject is performing a task followed by another set of image volumes when patient is at rest. This pattern is repeated a number of times. In voxel based analysis one then compare the voxel variance in time with the signal change expected from the task activation. Random motion during scans will induce a signal change that will be interpret as an extra source of noise and it will lead to a general drop in registered cortex activation due to lower signal to noise ratio. Since the signal change due to task activation is of the size of 0.5-5% a high SNR is crucial for a successful examination.

If the subject motion is correlated to the task paradigm, i.e. motion is present when there is a change between task/rest, it will lead to a signal change that is interpreted as task related activation. A low signal to noise ratio or high levels of false activation can render the fMRI data useless. In extreme cases as much as 90% of fMRI signal variation derives from motion 2].

A common way to deal with the effects of motion is to realign the image volume to a reference volume. The realignment is a rigid body translation and rotation around the x-, y-, z-axis. This is accomplished by a least square approximation, were the sum of all voxel difference between two images is minimized.

Statistical Parametric Mapping (SPM, Friston, K Web: http://www.fil.ion.ucl.ac.uk/spm/) is a voxel-based analysis method, which uses the General Linear Model (GLM) to describe the signal variation in the fMRI time series as effects modelled in a design matrix. Yet another way to deal with motion is to add the motion parameters estimated in the realignment procedure as effects of no interest (covariates) to the design matrix, it is possible that signal variation due to motion will be correctly interpreted as motion induced variance instead of as true activation.

SPM is sensitive to motion that is correlated to the task paradigm [3, 4]. In a case where the motion is well correlation, an SPM analysis with motion covariates as effects of no interest will not only fail to separate true activation from motion induced signal changes but it will also interpret true activation as motion induced signal.

One of our aims is to show when to add motion covariates and when not to.

1.1 Our suggested method

We suggest a method to remove motion induced variance in fMRI-signal by identifying motion variance and removing it by using a data driven method called Independent Component Analysis (ICA). ICA divides variance in fMRI time series into spatial activation maps (components) with voxels that share the same temporal variance. The temporal variance of each component will be compared to the estimated motion parameters in order to find

components that are well correlated to motion. Components with a high correlation to motion will be removed and the data will then be remixed. We will investigate if the ability to identify true activation will increase when artifactual signal variance is removed.

2. Theory

2.1 BOLD and fMRI physiology

Extrinsic connections between cortial regions are not continuously distributed around the region. Instead they occur in clusters. This suggests an anatomical and a functional segregation within cortex, i.e. neurons with the same functional properties are grouped together [6]. Therefore, useful information concerning brain function can be obtained using images with an in plane resolution ~3 mm. When a neural region is activated there is an increase in oxidative metabolism which leads to a greater local demand for oxygen. The neural activation is followed by an increase in blood flow in the adjacent region. In the 1890: s physiologist Charles Sherrington noticed that neural activation was followed by an increase of relative blood oxygen level following from the fact that the increase of local oxygenated blood due to the increase in blood flow exceeds the increase in oxygen utilization [7]. Deoxygenated and oxygenated blood has different magnetic properties, so a change in their relative concentration leads to a signal change; hence the signal is Blood Oxygen Level Dependent (BOLD). Typical signal change due to stimulation is 0.5 – 5% and it can be compared to the noise level of 0.5 – 1% [7].

Another common cause of fMRI signal change is subject motion. In a study performed by T. Krings et.al [1]., the result from 194 fRMI examinations were considered. Motion was found to be the most common cause for fMRI failure.

2.2 Generating fMRI time series

The fMRI data is generated by acquiring image volumes while the patient shifts between two cognitive states, e.g. task and rest. Analysis on the voxel values over time can track signal changes caused by the change from one state to another and eventually tell if a voxel contained activated neurons during the task.

The expected signal change due to task is not identical to the block paradigm. The true signal change for a single event (i.e. short period of activation) is described by the hemodynamic response time; which takes in to consideration all the physiological aspects, e.g. the few seconds of delay before one can see physical change in blood flow and blood oxygen level. The *expected task response* is modelled in SPM as the block paradigm convolved with the hemodynamic response, giving it the appearance seen in figure 1. This response is more likely to fit the true signal change in fMRI time series data.

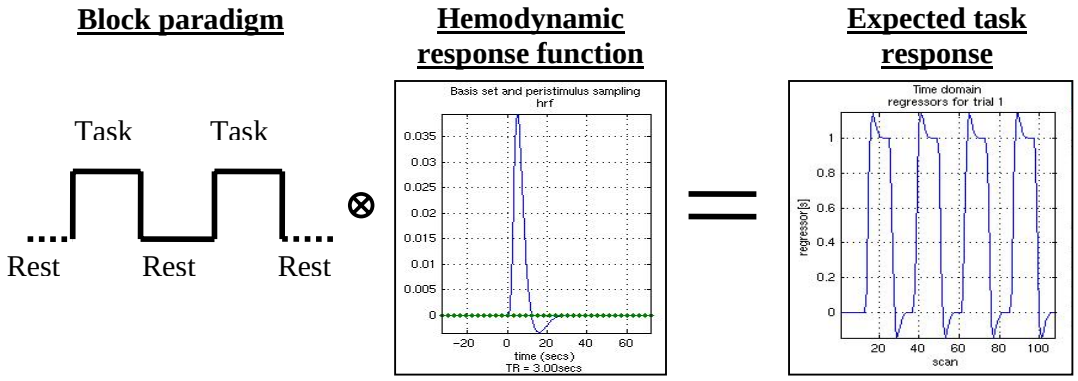

Figure 1, the block paradigm is convolved with the expected hemodynamic response of a single event. The result is the expected BOLD signal response with a duration of 190 of 10 images and onsets at 10, 30, 50 and 70.

To create a time series the voxel value that originates from the same spatial position over time is plotted as a function of time. The graph in figure 2 shows the variation in fMRI time series from simulated data were the red dots are voxel values from different time points in the data set and the grey line is the expected task response.

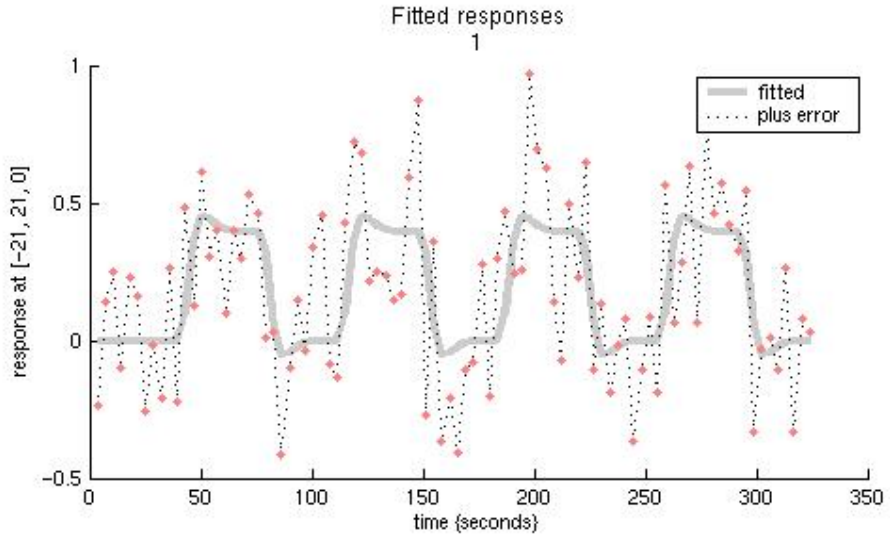

Figure 2. Variation in fMRI BOLD-signal in simulation data (motion correlation to task = 0.2 and motion = 1 mm). The red dots are voxel values at different times during the fMRI time series. The grey curve is the expected task response and the better the fit is between the two the more likely is it that the voxel will be considered activated.

2.3 The effects of subject motion

In an fMRI time series without subject motion present the signal value over time stems from the same anatomical volume. When motion is present the content of a voxel can change between two image acquisitions. This might lead to a signal change if the new voxel content has different magnetic properties than the previous content. If the voxel content in such situation is periodically entering and exiting the voxel with the same periodicity as the paradigm, i.e. movement when changing from one cognitive state to another, it will lead to a false activation due to the fact that the motion induced signal variation will be similar to the one expected from the true paradigm. These effects will be increased if a voxel is located at tissue boundaries were differences in magnetic properties are big at small distances.

All motion between image acquisitions affects the fMRI signal. There are two different ways in which this effect is manifested.

1. Motion that is uncorrelated with expected task paradigm will induce variance that is interpreted as an extra source of noise thus decreases the signal to noise ratio and making it difficult to detect true activation.
2. Stimulus correlated motion may create variance in image time series that are indistinguishable from true experimental changes.

To deal with the problem of head motion, a number of solutions are suggested.

2.4 How do we try to solve the problem today?

The first line of defence against head motion is to minimize it during exams. For this one uses foam padding, plaster head cast [8] and bite bars. Another approach is to do external motion measurement. A number of propositions have been made, like measurement of head motion with external optical motion tracking [19] and image based tracking [9] and then realign the images according to the obtained motion parameters.

More common is the image based realignment that is based on a "rigid body" approach, i.e. change in position and orientation without any shape change, where the images are realigned with a reference image. The reference image is often one image volume collected in the middle of the series. The realignment is a rigid body translation and rotation around the three coordinate axes $\left(x, y, z, \theta_x, \theta_y, \theta_z\right)$ and is based on a least square method. The differences between all spatially corresponding voxels are summarized over the two images. One images volume is the translated and rotated until the sum of squares between two images, I and P, is minimized

$$\min = \sum \left(I_{x,y,z} - P_{x,y,z} \right)^2 \qquad (2\text{-}1)$$

The realignment gives an estimation of the patient's movement. The estimated motion translation and rotation parameters can later be used in the general linear model as effects of no interest.

Even in absence of subject motion, when activation is present in a number of image volumes, studies show that the realignment might induce false activation because of the variance caused by task induced activation [10].

Even after a perfect realignment there can still be signal changes derived from motion due to the spin history effect [2]. To what extent the spins (protons) is excited are decided by the interaction between the local magnetic field and the slice selective pulse. Spins that are close to a slice boundary are very sensitive to displacement in and out of the slice. If the number of excited spins depends on the position of the spin, the number of excited spins also depends on the previous positions of the spins. This is due to the fact that the saturation of spin magnetization is dependent on the number of excitation in previous scans. The spin history effect can be present when the repetition time is similar to the T1-relaxation time.

2.5 SPM

Statistical Parametric Mapping (SPM) is often used to analyze fMRI data. SPM uses the general linear model to estimate regional effects. The goal is to represent image time series

data as a linear combination of explanatory effects and an error term. The general linear model can eliminate effects, like general movement and respiratory movement provided that the effects can be estimated or measured.

2.5.1 General linear model

As a part in the general linear model there is a *design matrix*, G that accounts for all the neurophysiological effects on the response (task response, dummy variable representing mean signal). A model with these two effects alone can be successful in identifying true activation. But as previously mentioned; motion that is correlated with the task paradigm can cause spurious activation.

To tackle the effects of correlated motion it is possible to add the estimated motion parameters from the realignment process as "effects of no interest" (covariates). If there is motion induced variance present in the fMRI time series then this variance can be modelled by these covariates. The design matrix, G, has one row for every image volume and one column for every effect.

$$\overline{X} = G\overline{\beta} + \overline{\varepsilon} \qquad (2\text{-}2)$$

β is a one row vector were one value corresponds to each effect. This value is the estimated amplitude of the corresponding effect, e.g., to which extent β:s corresponding effect models the signal variance. ε is a matrix of normally distributed error terms, i.e. effects that can not be explained as effects modelled in the design matrix.

X is a matrix with the fMRI time series of observed voxel values. It has one column for each voxel and a row for every scan. Two different design matrixes are pictured in figure 3 were the left panel shows the design matrix that consists of expected task response and the dummy variable, and the right panel shows a design matrix with motion parameters as effects of no interest.

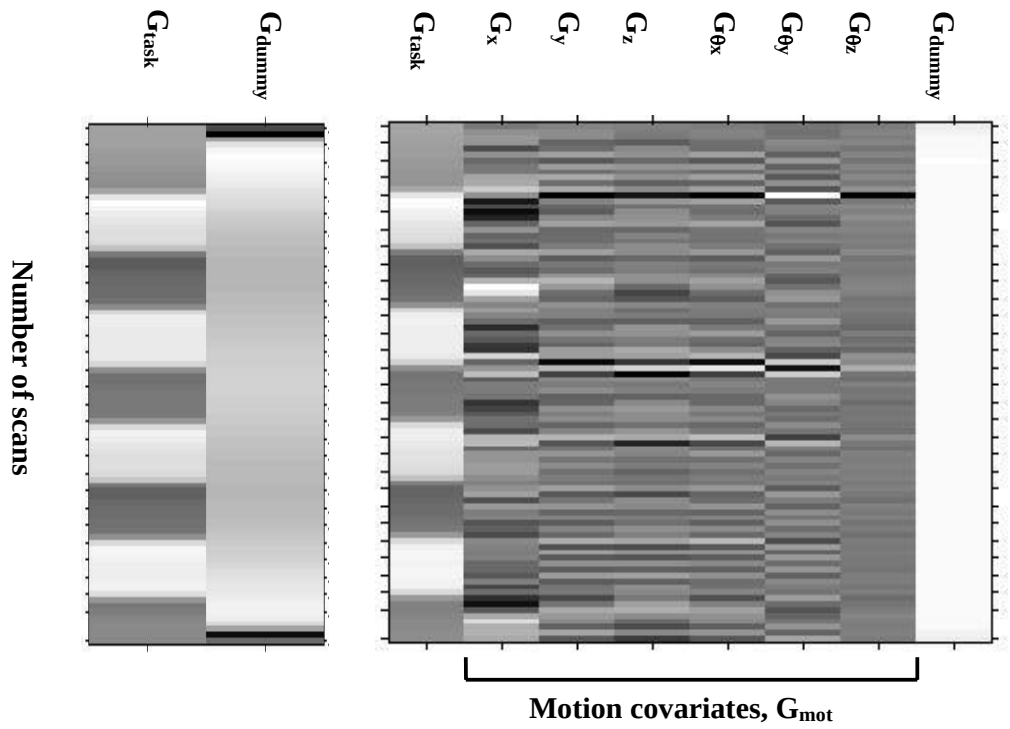

Figure 3, two different design matrixes, one with motion covariates (right) and one without (left). The number of scans is 90, hence 90 rows. In the matrixes the left explanatory variable describes the expected task response and the right is a dummy variable that consist of only ones. In the right matrix, the six middle covariates are the motion parameters added as effects of no interest. The fact that the dummy variable in the left matrix isn't entirely white is because there is a small deviation from one at the edges. These deviations are so small that they will not greatly affect the outcome of the analysis.

The first covariate G_{task} describes the task induced deviance from the mean signal. The last covariate G_{dummy} is a dummy variable that accounts for the mean signal strength. The six middle covariates are the estimated motion parameters added to the design matrix to separate task induced signal change from motion induced.

By adding motion covariates another problem may be introduced. This is if motion, let say translation on the x-axis is well correlated with stimuli, the covariate G_{task} will be similar to the covariate $G_{\text{trans-x}}$; hence they will model a similar signal variation. The result of this double modelling can be that true task induced variation is interpreted as motion induced and vice versa.

Including the motion parameters as effects of no interest can one hand lower the amount of voxels falsely activated but on the other hand also cause loss of true signal when the correlation between the motion and task is too high.

2.5.2 t-statistics

The detailed mathematics of the t-statistic is well beyond the scope of this thesis and the theory presented here gives a very simplified picture of the theory. Readers are referred to reference 20 for more detailed information. t-statistics is a measure of how well the signal variance in a voxel time series concurs with the expected task response. The t-value is the ratio between the amplitude of the expected task response, $\beta_{response}$ and the residual variance (error term).

If a major part of the voxel signal variance is interpreted as variation due to stimulation $\beta_{response}$ will be high and the *t-value* for that voxel position will be high. A t-value is calculated for every voxel position inside the brain, thus creating a *t-map*. These t-maps describe how well each voxel variance is modelled by the expected task response function.

2.6 Independent component analysis (ICA)

2.6.1 Introduction

As previously mentioned the signal variance in fMRI time series depends on different effects and properties, e.g. noise, motion and BOLD stimuli. The registered signal variance is a combination of these effects. Theses effects can be represented by one or several spatially independent components, each associated with its own time series. Independent component analysis (ICA) tries to separate the different signal variation that origin from different effects.

ICA can locate voxels that share the same variance in time. One can roughly say that they stem from the same physical effect. By comparing the temporal signal variance in every component with the estimated motion parameters one could hope to find the component representing motion induced signal change.

Any given component can be removed and the data can be remixed without the signal variance described in that component. In theory, if one can identify the components representing motion induced signal variance, the component could be removed and the motion free data could be remixed before analysis. Next follows a brief explanation of the ICA model.

2.6.2 The ICA model

ICA decomposes the fMRI data component maps into spatially independent component maps without knowing anything about their spatial distribution or time course. The source data are assumed to be non-Gaussian and statistically independent, i.e., one component does not provide any information about other components. The independent component maps **S** can, roughly speaking, represent different physical effects, e.g., BOLD response and motion. The acquired fMRI voxel time series **X** is modelled as the component maps **S** mixed by an unknown mixing matrix **A**;

$$X = AS \qquad (2\text{-}4)$$

To solve this problem with two unknown variables the mixing matrix must be estimated. The components can be extracted using the inverse mixing matrix (or the unmixing matrix) $A^{-1} = W$. The spatially independent maps will be acquired trough

$$S = WX \qquad (2\text{-}6)$$

The unmixing matrix is estimated in two steps. First, the number of components must be limited, this process is called whitening. Whitening arranges the data into Principal Components according to the amplitude of their variance and components with small variance amplitude are excluded. The second step involves identifying the independent components and extracting them from the data using an algorithm. There are several ways to estimate the component independence, e.g., maximization of non-Gaussianity and Maximum Likelihood Estimation (MLE). The component variance can be excluded from the fMRI variance by assigning the corresponding time course in **W** as zeros. The data can be rebuilt again without the component contribution to fMRI variance.

In this thesis we used GIFT [12] tool box for MatLab which uses the INFOMAX algorithm [11].

Previous studies have shown a promising potential for removal of motion induced variance with ICA [13] and as result increase the analysis sensitivity and specificity.

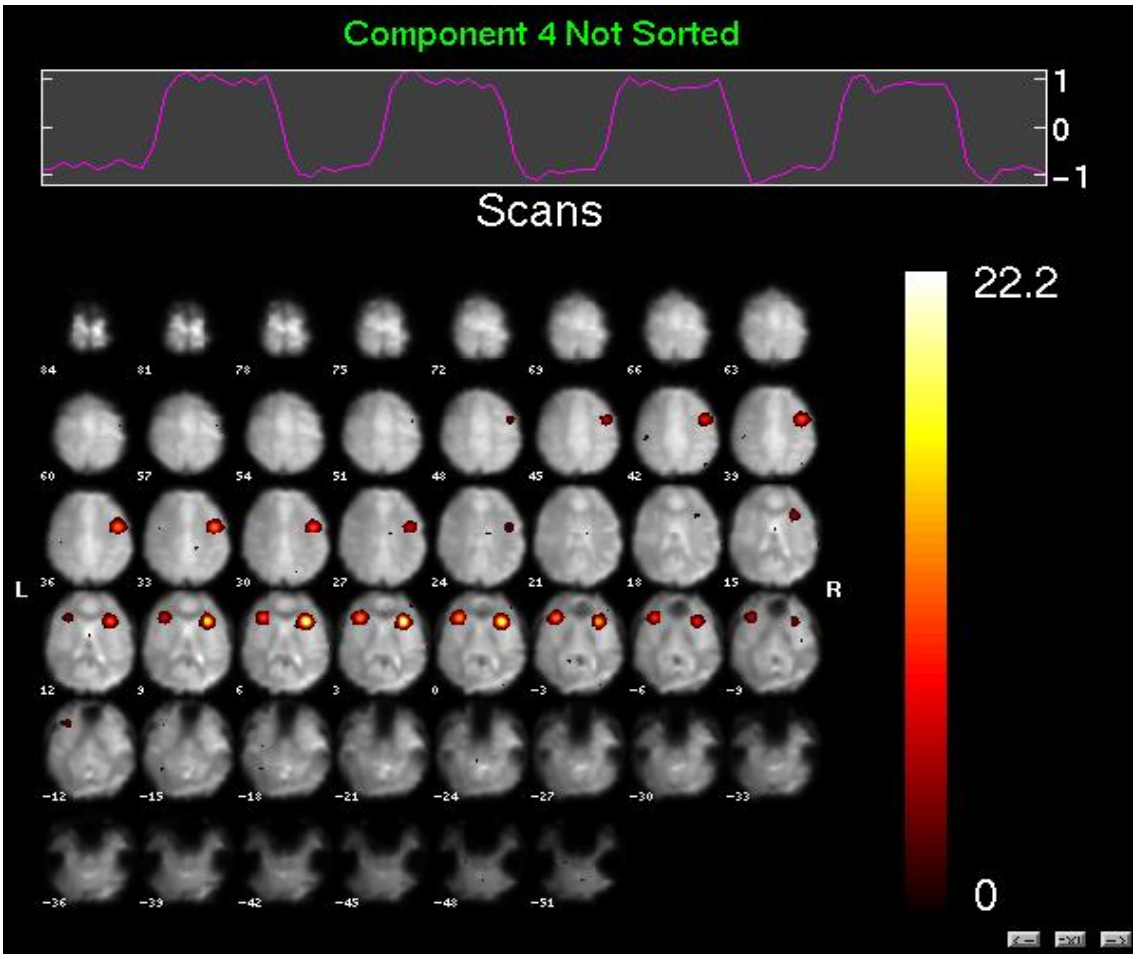

Figure 4. One components from simulated data (correlation to task is 0.5 and simulated motion size is 1 mm) separated by GIFT [12] using the Infomax algorithm. The image shows the spatial distribution and time course for simulated BOLD induced variance.

3. Material and method

Both patient and simulated data were used to investigate motion induced effects artefacts in fMRI time series. The examinations were conducted using a GE 3T scanner. The data consist of an image volume (*.img) and a header (*.hdr) with information about each image volume (e.g. patient info, examination parameters and location in image time serie).

3.1 Simulated data

Simulated data with known motion size and correlation to task were created. Simulated data has the advantage that the ground truth is known and it is possible to compare the analysis result to the true activation. A simulated image time series was created by copying and renaming a single normalized image volume, resulting in an fMRI time series with a total of

90 scans (TR: 3.6 seconds, 60 degrees flip angle, 128x128, slice thickness: 4 mm, pixel size (x, y) 1.88 mm).

Gaussian distributed noise was added to all image volumes in order to mimic the noise present in a true time series. The standard deviation was set to 2.5% of mean cerebral voxel value [10]. These image volumes were used as base data set. 16 different data sets time series were created by applying different combinations of activation, motion size and motion correlation to the base image volumes.

Table 1 is shows the all the different parameter combinations used.

Activation (%)	Motion size (mm)	Motion correlation	Number of data sets #
1, 3, 4, 5	~1	0.5	4
2	~0.1; ~1; ~5; ~10 (x-axis translation)	0.2; 0.5; 0.8	12

Table 1. The combination of parameters used to create all the different simulated data sets.

3.1.1 Activation

3 spheres (blobs) of activation were added to the base image with five different activation sizes; 1, 2, 3, 4, 5 (%) of mean signal. The blobs were weighted, e.g., at 5% signal change blob 1 had 5% signal change, the second blob 4% (80%) and the last blob 3% (60%). Their spatial position and respective weight are presented in table 2 below and the spatial distribution is seen in figure 5. The temporal distribution was a repeated sequence with 10 image volumes with no added activation followed by 10 with activation. The onsets were image volume 10, 30, 50 and 70 and the duration of the activation was 10 image volumes long.

Blob number	Weight	x	y	z
1	1	-34	20	2
2	0,8	36	28	0
3	0,6	-46	0	34

Table 2, the brain coordinates (mm) for the added simulated activation blobs

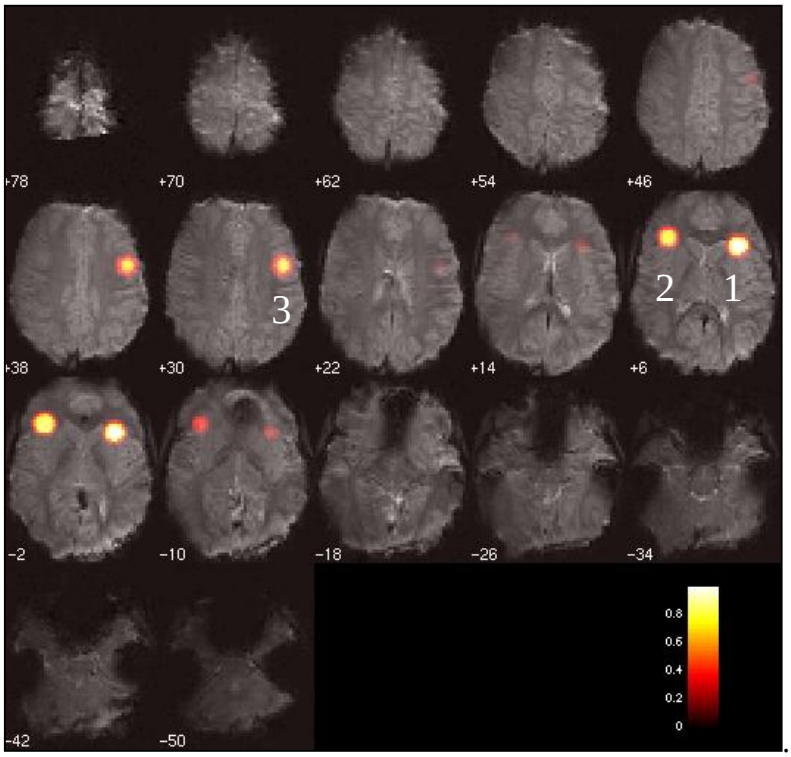

Figure 5, Gaussian distributed spherical activation blobs was added to the image set with a total of 90 images. The duration was 10 image volumes long and the onset was image 10, 30, 50, and 70.

3.1.2 Motion size and correlation

Motion must be added to the simulation data in such way that the motion and stimuli-correlation is known.

We created a motion schedule with known size and correlation to task by adding noise to the expected task response as shown in figure 6a. In this way we created a motion schedule with a correlation coefficient 0.8 between the motion schedule and expected task response. To simulate a motion schedule with correlation coefficients of 0.5 and 0.2 the expected task response was modified as seen in figure 6b were two (upper) and three (lower) of the task blocks were removed before the noise was added. The correlation between the added motion and the expected task response is nominated as cc_{mot}.

To model different motion sizes (0.1, 1, 5 and 10 mm), the individual motion schedule was multiplied by 0.1, 1, 5 and 10.

Each image volume was then translated according to the given translation in the motion schedule. Motion was only added as translation along the x-axis. Each image volume was moved according to the corresponding value in the motion schedule using the SPM reslice option.

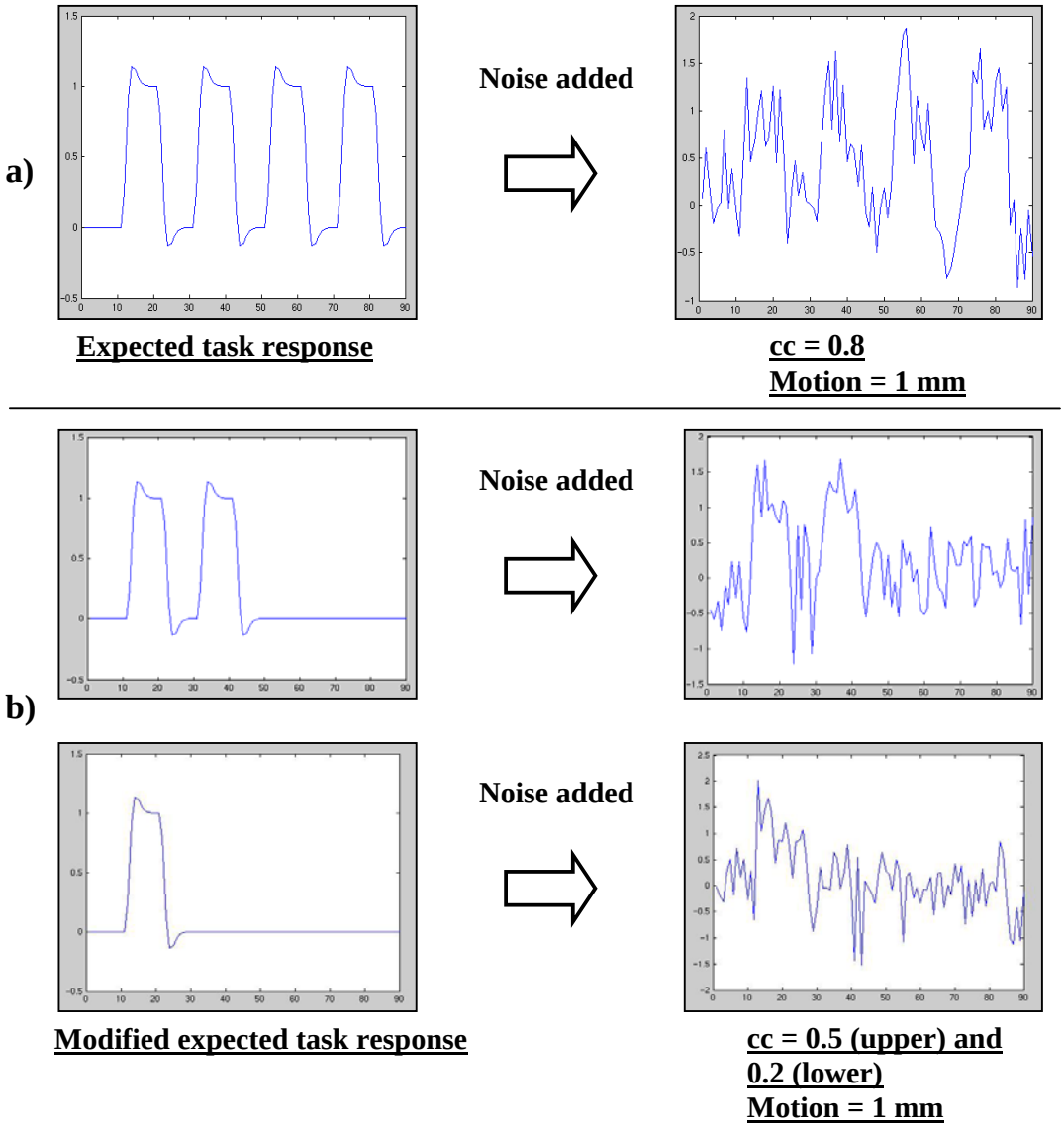

Figure 6. Motion correlated to task. Noise was added to the expected response to simulate different correlations. To simulate low correlated motion the expected task response was modified before noise was added. Two of the stimulus "blocks" were removed before noise was added to create a 0.5 correlation between motion and task. To simulate a correlation between motion and task of 0.2 all but one stimulus block was removed.

3.2 Patient data

We used patient data from 34 healthy volunteers. All 34 patients had performed an orthographic lexical retrieval (OLR) examination. While in the scanner they were asked to generate words starting with a letter displayed on a screen, the letter changed after 18 seconds. During the rest state the patient was asked to focus on a cross-hair. The paradigm consisted of four blocks with 36 seconds rest and 36 seconds word generating (task). Images were acquired with two different pulse sequence parameters seen in table 3.

Number of subjects	Repetition/Eco time, TR/TE seconds	Flip angle	Resolution	Number of scans	Number of slices	Slice thickness	Pixel size
16	3.6 / 0.04	60	128x128	90	25	4 mm	1.88 mm
18	3.0 / 0.04	75	64x64	107-111	36	3 mm	3.45 mm

Table 3. Image parameters for all patient data. All images were acquired with a gradient echo-planar imaging sequence.

A way to quantify subject motion is to estimate the mean translation between image volumes d_{mean} using the estimated motion parameters from realignment. d_{mean} is the squared difference of estimated motion between two image volumes in all dimensions divided by the total number of images volumes minus one.

$$d_{mean} = \frac{\sum_{i=1}^{N} \sqrt{\left(\left(x_i - x_{i+1}\right)^2 + \left(y_i - y_{i+1}\right)^2 + \left(z_i - z_{i+1}\right)^2\right)}}{\text{N-1}} \qquad (3\text{-}1)$$

N is the total number of image volumes that are acquired during the scan and x, y and z are translation in respective direction between image acquisition. The effects of motion between image acquisition can be investigated by plotting analysis performance as a function of d_{mean}.

3.3 Pre-processing

All image time series where pre-processed before they were analyzed and evaluated. The pre-processing involved, in order of implementation; slice timing, realignment, smoothing and normalization.

3.4 Analysis

5 different analysis procedures are considered.

1. Analysis with motion parameters as covariates (MC)
2. Analysis without using motion parameters as covariates (NoMC)
3. Analysis on data sets were the component with the highest correlation to motion is removed (ICA1) from the data sets. During the analysis motion parameters were used as covariates.
4. Components with a correlation to motion higher than 0.3 were removed from the data sets. Motion parameters as covariates were used during the analysis.
5. Components that had a correlation to motion higher than 0.3 and a correlation to task response lower than 0.3 were removed. Motion parameters were used as covariates during the analysis.

For procedures 1 and 2 one uses SPM2 directly on the pre-processed image data.

In 3, 4 and 5 the fMRI time series data were divided into independent components by using GIFT [12], each component associated with an individual time serie. GIFT uses the algorithm Infomax, which is described in literature as robust and highly accurate [11].

The individual time serie of each component was compared to the motion parameters, i.e., producing a correlation coefficient between the two. A component (or components) with high correlation to motion can be removed and data analyzed with out its contribution to the signal

variance. We used three different criterions for selecting motion components. Data with components removed according to the first criterion will be labelled ICA1 and with the second criterion ICA2 etc.

In the data set called *ICA1*, the pre-processed data was analyzed using GIFT, and the component with highest correlation to motion was removed. Our assumption is that this component is the most likely to represent motion induced signal variance.

This assumption might be a bit to inaccurate when perhaps several components contribute to motion induced signal variance. Therefore in *ICA2* data sets all components with motion correlation to task higher than 0.3 was rejected. This threshold is referred to as the *motion rejection threshold*.

The third scenario is when motion is well correlated with the expected response. If GIFT is sensitive enough to separate stimuli induced variance from motion induced variance, these two components will have similar time series. With the two previous selection criterions there is an obvious risk that stimuli induced variance can be interpret as motion induced, and therefore eliminated.

The components removed from *ICA3* data must have a correlation between its time serie and motion parameters higher than 0.3 but also a correlation to expected task response less than 0.3. Both these demands must be satisfied for the component to be removed, hence giving a better protection against removal of true activation but unfortunately also decreasing the sensitivity for removal of correlated motion.

ICA data were then analyzed by SPM with motion covariates as effects of no interest. Some simulated data were also analyzed without motion covariates in GLM to investigate the effect of adding covariates or not when analysing ICA data.

3.5 Evaluation

Three different evaluation methods were used on our analyzed data sets.

1. area under ROC (*auROC*) curve
2. t-ratio
3. Goodness of fit

For simulated data the ground truth is know. This makes the data suitable for auROC evaluation (area under Receiver Operator Characteristic curves) which is a comparison between true positives and false positives.

The t-ratio is an alternative method for evaluating patient data in which the ground truth is unknown. To test the validity of the t-ratio evaluation method we compared results from simulated data with the acknowledged auROC evaluation [14, 15, 16]. If the two evaluation methods produce similar results, the results based on a t-ratio evaluation can be better justified.

Both simulated and patient data were evaluated using goodness of fit.

SPM2 creates a t-map with t-scores for every voxel inside the brain. A high t-score indicates that the voxel signal variation is well described by the expected task response. These t-maps are used to evaluate our analysis results.

3.5.1 Area under ROC

When the ground truth is known, as in our simulated data, it is possible to study the relationship between the number of true positives and false positives. This makes simulated data suitable for an auROC evaluation.

Figure 8 displays the ROI:s used for the evaluation of simulated data. The red volume is the spatial distribution of the added activation blobs and the green is the brain volume. The blue

volume is the difference between the activation volume and a smoothed version of the activation volume. t-values from the blue ROI was excluded from the evaluation because there was an increase in t_{out} close to the activation ROI border when the activation amplitude (% of mean signal) increased. After the smoothing process during the pre-processing step, some parts of the added activation blobs are located outside the original boundaries. They will cause an unwanted raise in t-value just outside the activation ROI, t_{out}. These t-values are not false in the sense that they stem from true activation, neither are they true because they are outside the added activation ROI.

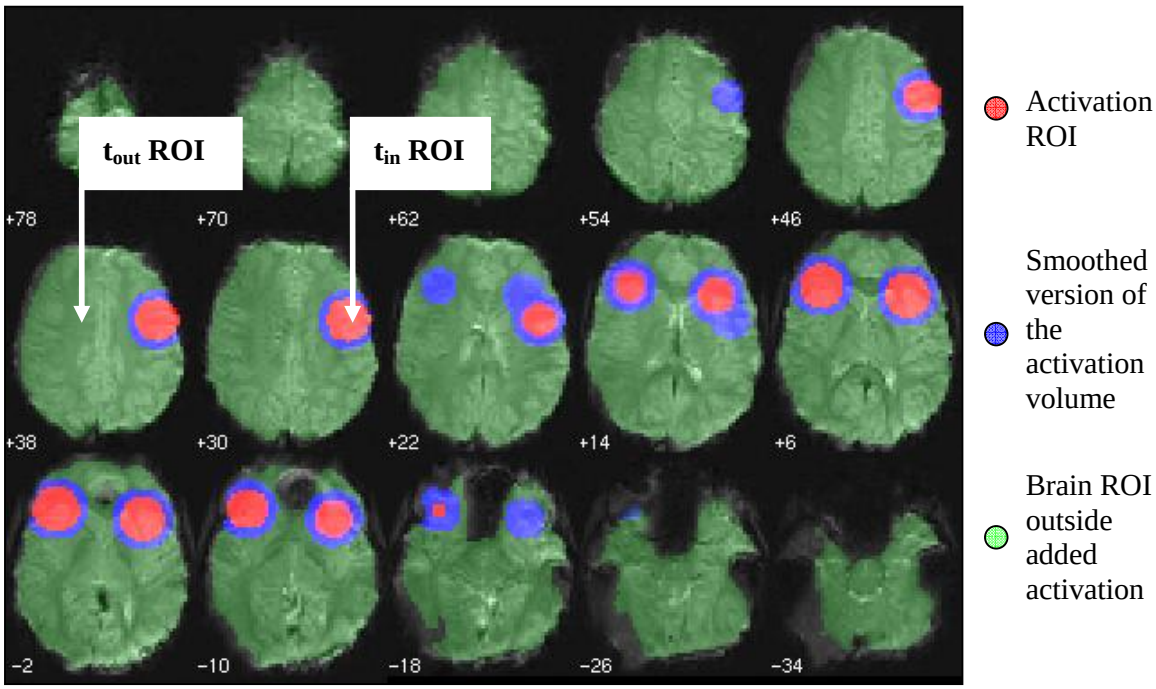

Figure 7. Spatial distribution of ROI:s used to calculate auROC for simulated data. The ROI:s are displayed on one of the pre-processed images. Red ROI is equivalent to the volume of the added simulated activation blobs, blue ROI is a smoothed version of red ROI and green ROI is the brain except the smoothed simulated blobs.

To create a ROC curve the ground truth must be know. In such cases it is possible to compare the analysis results to the known truth. The curve is generated by the two coordinates given in eq 3-2 and 3-3.

The True Positive Fraction, *TPF* is the quotient between the number of activated voxels in the red ROI and the total number of voxels in the same ROI.

$$TPF(t) = \frac{\text{number of voxels in activation ROI above t-threshold}}{\text{number of voxels in activation ROI}} \qquad (3\text{-}2)$$

The False Positive Fraction, *FPF* is the ratio between the number of voxels in the brain ROI that exceeds the threshold *t* and the number of voxels outside the brain ROI.

$$FPF(t) = \frac{\text{number of voxels in brain ROI above t-threshold}}{\text{number of voxels in brain ROI}} \qquad (3\text{-}3)$$

An ROC (receiver operator characteristic) curve were generated by the two coordinates TPF(t) and FPF(t) at different t-thresholds. An ROC curve displayed in fig 9. The TPF(t) (y-axis) and FPF(t) (x-axis) was acquired between t = 0.1,…, 20 in steps of 0.1.

The results from an ROC curve can be summarized and described by the area under ROC curve (auROC). auROC is a measure of the method performance were a high auROC indicates a good analysis performance (high TPF and low FPF).

The area under the ROC was integrated from FPF = 0 to FPF = 0.1 using a cubic spline interpolant (spline command in Matlab).

3.5.2 t-ratio

The t-ratio is a measure of the sensitivity and specificity of the analysis. To find the appropriate t-values for the t-ratio evaluation the ROI:s displayed in figure 8 were used. The t-ratio is

$$t-ratio = \frac{t_{in}}{t_{out}} \qquad (3\text{-}4)$$

were t_{in} is the highest t-value inside the red ROI. If an OLR examination is preformed the activation is likely to occur inside the red ROI [18]. t_{out} is the highest t-value inside the green ROI. The green ROI represents the volume were no activation is expected. Also displayed in figure 8 is the lingual activation in two healthy volunteers (OLR). The ROIs are generated from 30 volunteers. To select the ROI regions the four voxels with highest t-score was chosen. Around these voxel a spherical volume (5 mm diameter) was centred. This ROI is represented by the red colour in the lower image in figure 8.

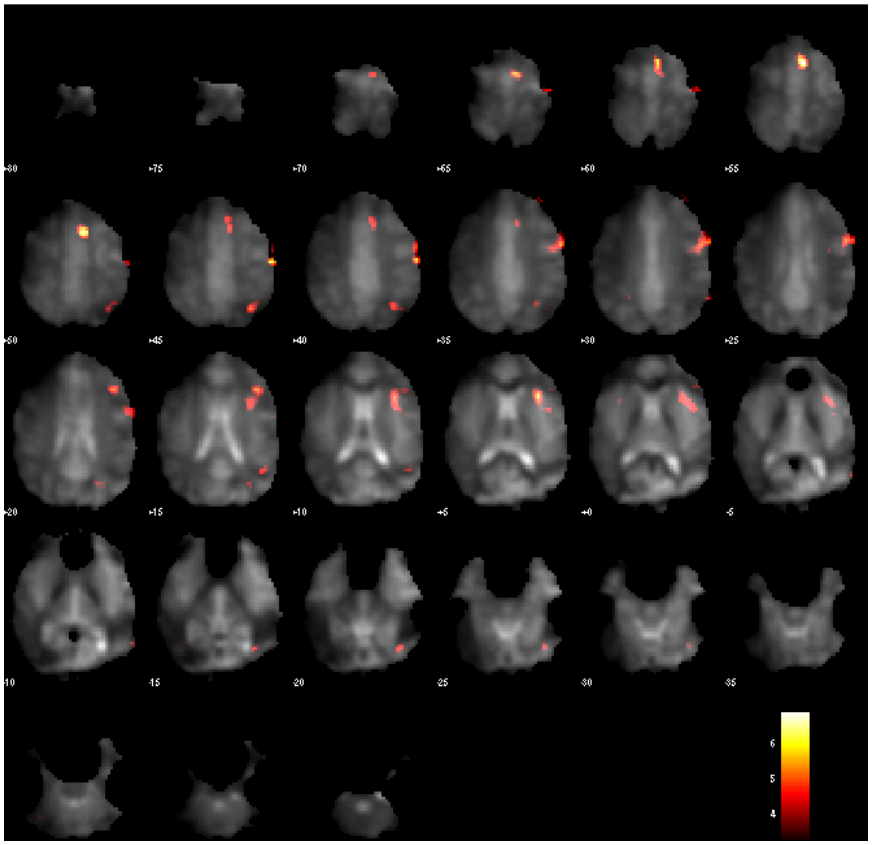

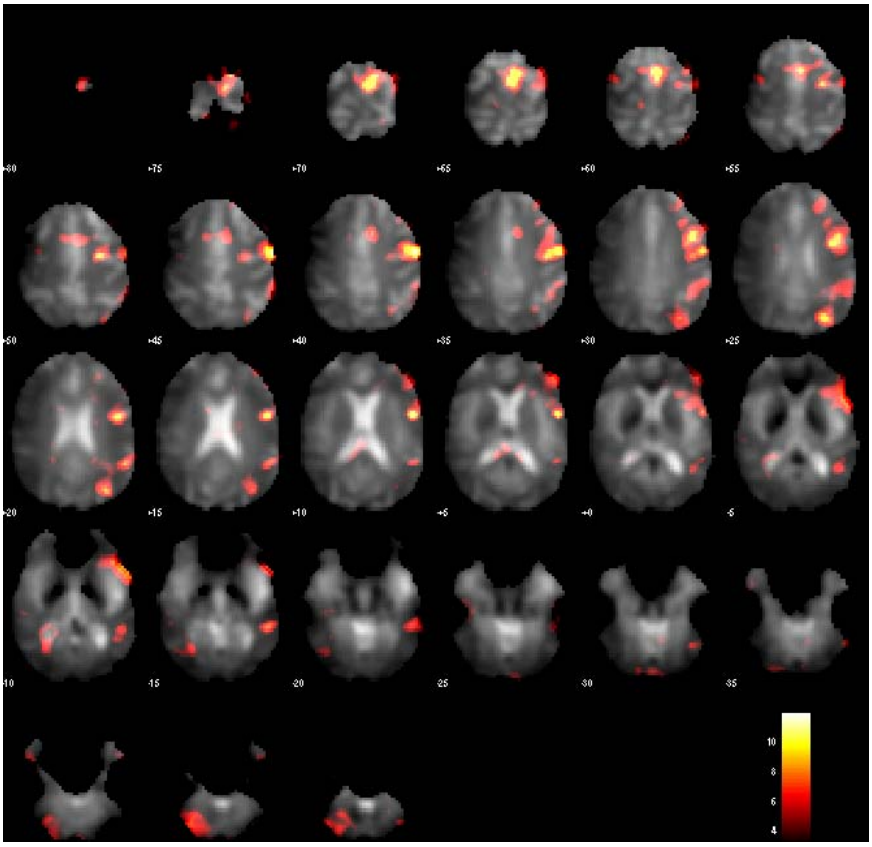

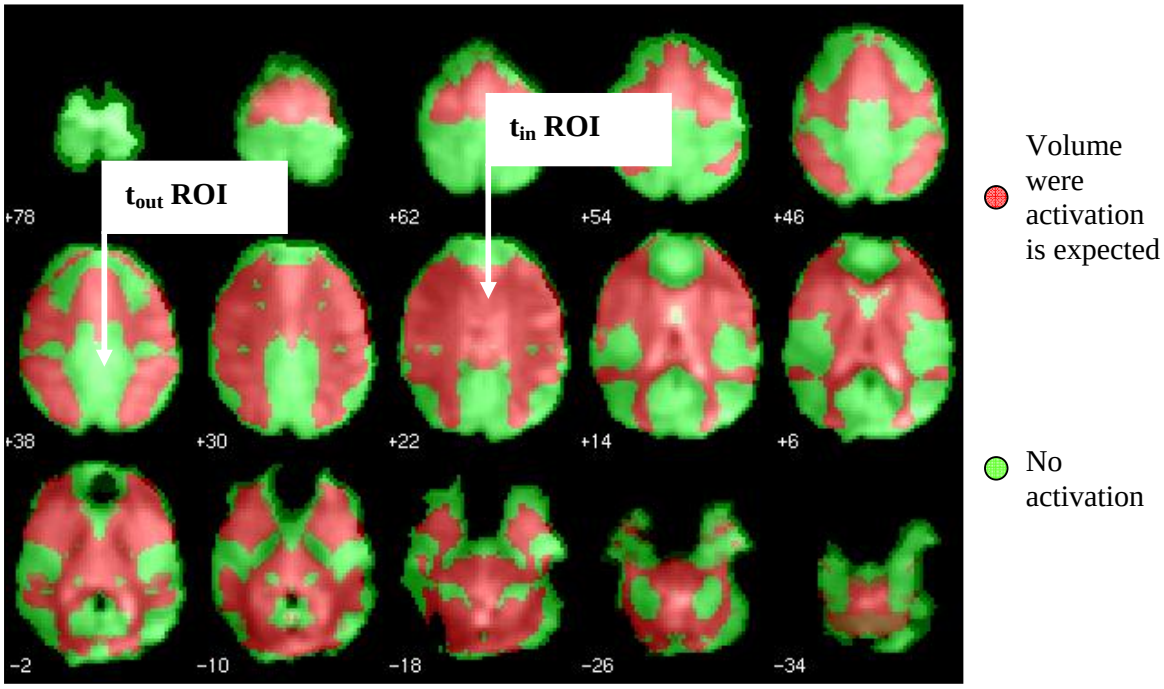

Figure 8. Top and middle: Registered activation (t < 3.2) in a healthy volunteers. Bottom: The spatial distribution of the ROI:s used to calculating t-ratio patient data. The ROIs was generated using the healthy volunteers. Red ROI represents a volume were one would expect activation from a language task. Green ROI is the brain volume except red ROI.

3.5.3 Goodness of fit

In t-ratio evaluation one draw conclusions about data from the maximum t-value inside activation ROI and brain ROI. This approach may give misleading information, e.g. in cases when the subject has not fully complied with the stimulus paradigm no activation is expected, but false activation can still occur due to artefacts, hence misleadingly implying that one method is better than another. To evaluate data without having this problem a third evaluation method was used.

The goodness of fit describes how well the data is described by the model, i.e. in our case; how much of the total variance that is described by the task covariate in the general linear model. The following notations are adapted from Waites et.al. [17]. The goodness of fit can be described by the coefficient of determination R^2.

$$R^2 = 1 - \frac{\sum\left(Y - \hat{Y}\right)^2}{\sum\left(Y - \bar{Y}\right)^2} = \frac{SSE}{SST} \qquad (3\text{-}5)$$

were Y is fMRI time series, $\bar{Y}$ is the mean fMRI signal and $\hat{Y}$ is the modelled estimate of Y. The sums are known as sum of squared error (SSE) and total sum of squares (SST).

By adding more covariates to the General Linear Model it is possible to better model the data, hence increasing the goodness of fit. To add more covariates can lead to an over fitting of the data. This is a problem when comparing results between analysis with and without motion covariates. To avoid this problem we used the adjusted R^2, $\left(R_a^2\right)$ which will adjust for the extra set of covariates used in analysis with motion covariates.

$$R_a^2 = 1 - \frac{SSE/\left(n-k-1\right)}{SST/\left(n-1\right)} \qquad (3\text{-}6)$$

n is the number of independent observations (number of images), k is the number of explanatory effects in the model. An R_a^2 value at 1 is a model that perfectly describes the data variance, and a R_a^2 value at 0 is a model that doesn't explain the data variance at all. A R_a^2 brain map was generated for MC, NoMC and ICA1. An example; to compare different models we subtracted $R_a^2\left(NoMC\right)$ brain volume from the $R_a^2\left(MC\right)$ brain volume and created an ΔR_a^2 image volume. The ΔR_a^2 image volume is referred to as a *difference in goodness of fit map*. All voxels with a negative value would indicate that NoMC best models the data and positive value would suggest MC. The mean value over the ΔR_a^2 image volume would tell us which of the methods that generally describes the data best. A positive value would mean that the MC is better at describing data and a vice versa.

An ΔR_a^2 image was also created for MC and ICA1.

For simulated data the mean values of the ΔR_a^2 images were plotted as a function of correlation coefficient, motion size and activation amplitude. For patient data the ΔR_a^2 mean value is presented for each individual subject.

4. Results

4.1 Simulated data

ICA2 and ICA3 identified the same components as being motion related in all simulated data. Therefore in the figures both methods are represented by the same graph (ICA2+3).

4.1.1 Area under ROC

A point on the ROC (Receiver Operator Characteristic) is determined by the number of true and false positive voxel at a certain threshold t. The curve is generated by plotting the TPF and FPF at different t-thresholds (0,1 -20 in steps of 0.1).

The auROC (area under the ROC curve) is a one variable that describes the performance of the different analysis methods. The area was integrated from 0 to 0.1 [14] and a performance close to 0.1 means that the method is successful in identifying true activation without any false activation. In figure 9 the part of the ROC curve that was used for auROC is displayed.

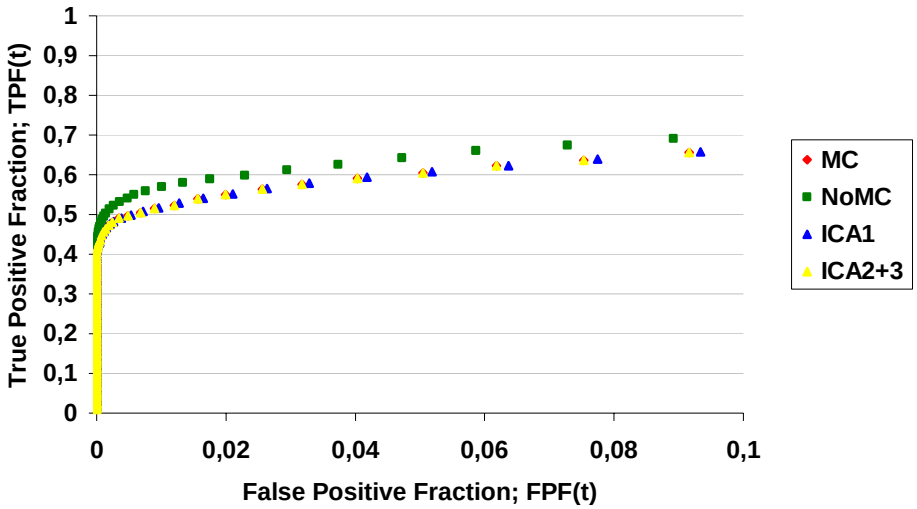

Figure 9. Receiver operator characteristics for simulated data with motion size 0.1 mm and the correlation between motion and expected task response is 0.2.

Area under ROC as a function of motion size

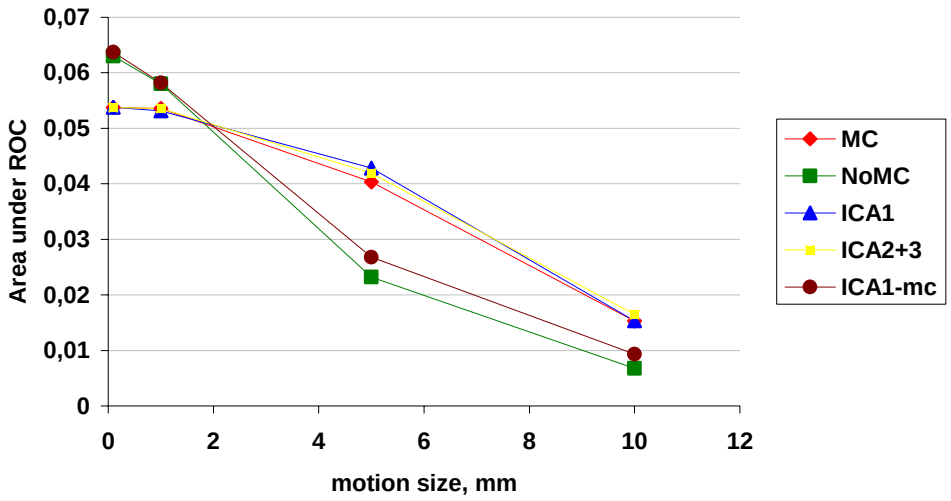

Figure 10. AuROC as a function of different motion sizes on simulated data. The correlation between motion and expected task response is 0.8.

In figure 10 the data shows that all methods perform worse when motion increases. When motion is low or moderate in size (<2 mm) NoMC performs better but when motion increases to 5 and 10 mm the relationship is the opposite. Notice that the lines cross at 2 mm, MC is the better method on the right side and NoMC on the left side.

ICA and MC performs similar and ICA can not successfully remove motion induced effects.

The extra method shown in figure 10 is from an analysis on ICA1 data without motion parameters as covariates in the design matrix. Excluding covariates in the GLM does not affect the analysis performance on ICA1 data to any greater extent.

Below in figure 11 is the same data evaluated using t-ratio as a measure of the success of each method in identifying true activation.

The results from figure 10 (auROC) and 11 (t-ratio) are from the same data sets but different evaluation methods. The graphs share some features, e.g. both the auROC and the t-ratio decrease when motion size increases. Another feature they got in common is that NoMC is less effective when motion increases. These shared features indicates that the t-ratio can be used for patient data were an auROC isn't possible.

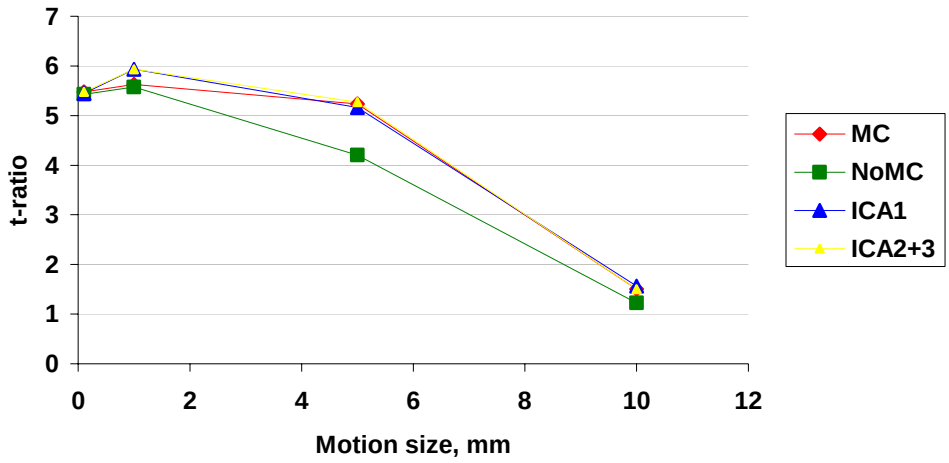

Figure 11. t-ratio as a function of motion size. The behaviour of the t-ratio curves is similar to the ones in auROC which would suggest that t-ratio also is a robust evaluation method and can be used to evaluate patient data without a know ground truth.

Area under ROC as a function of correlation coefficient

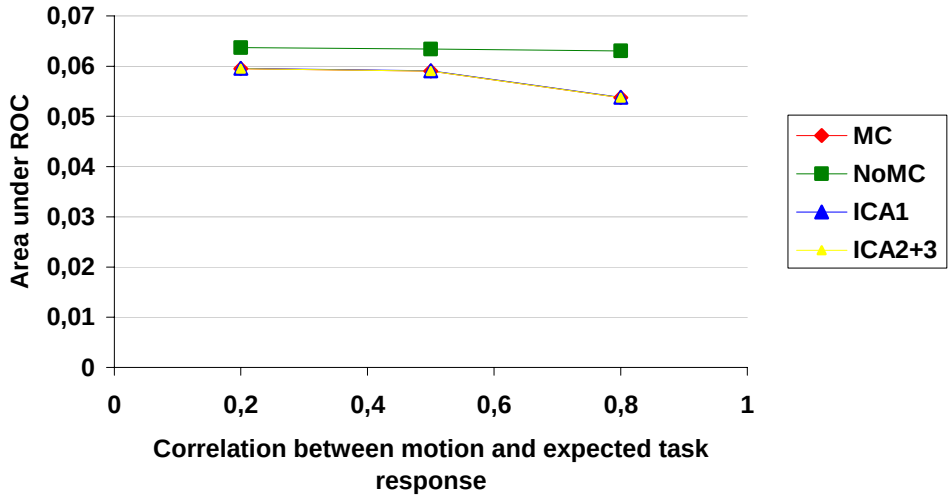

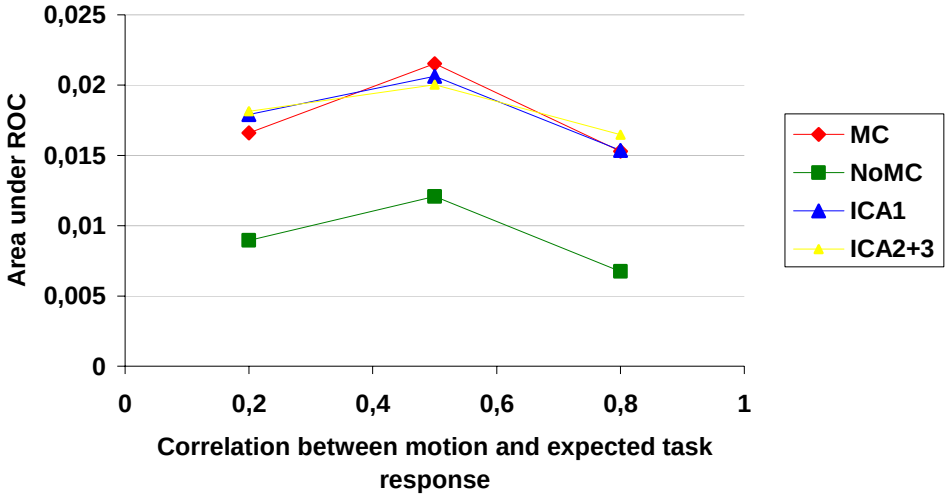

Figure 12. AuROC for motion 0.1 mm (upper) and 10 mm (lower). On y-axis is the auROC and on the x-axis is correlation coefficient between motion and expected task response.

In figure 12 the performance of the methods are plotted against the correlation between motion and expected task response. A high auROC-value suggests that the method is successful in identifying true activation. The upper graph is the results from data sets with 0.1 mm motion added and the lower is 10 mm motion added.

From both of the graphs the same conclusion is drawn; that the relative performance is constant and independent of correlation to motion.

There is no major difference between MC and the ICA methods. NoMC performs slightly better when subject motion is low or moderate (< 2 mm). At higher levels of motion (> 2 mm) MC and ICA is more successful at identifying true activation.

Area under ROC as a function of signal amplitude

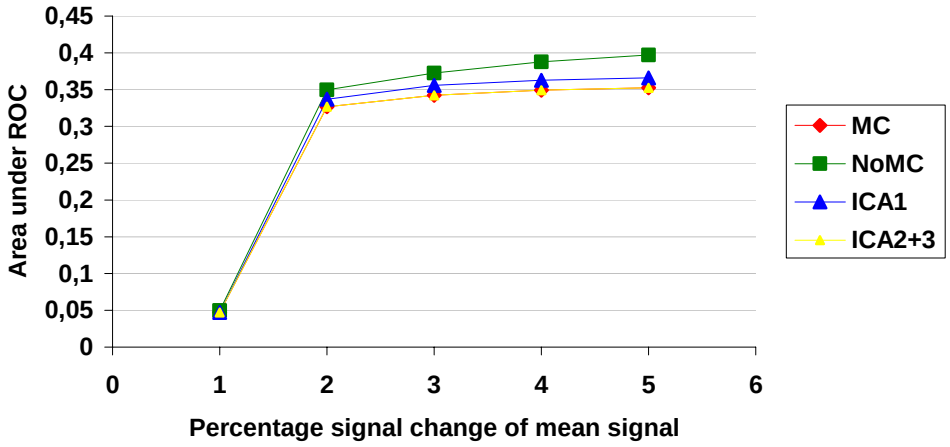

Figure 13. AuROC(%) with motion size 1 mm and motion correlation to expected task response is 0.5.

In figure 13 is the auROC as a function of percentage signal change. Five different signal changes were simulated, 1-5 %.

The auROC increases when the signal strength increases from 1% to 2%. Further increase in signal strength doesn't significantly affect the auROC.

The methods produce similar results and they all behave similar when signal strength is increased. NoMC is a slightly better at identifying true activation, especially at higher levels of activation but not to any greater extent.

4.1.2 Goodness of fit

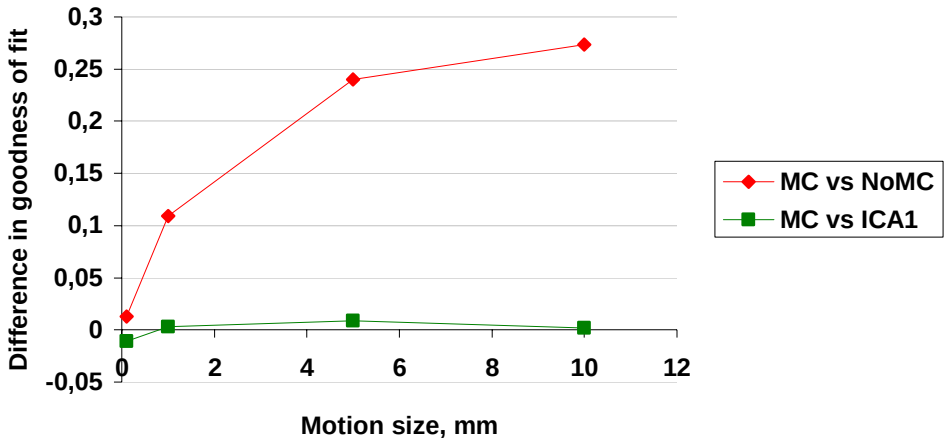

Figure 14. Difference in Goodness of between MC and both NoMC and ICA1 for different motion sizes. The correlation between motion and expected task response is 0.2. Positive value on the 'difference in goodness to fit'-axis suggests that MC is more successful in describing the data while a negative would suggest the opposite.

Figure 14 shows the relation between difference in goodness to fit and motion size. The goodness of fit was acquired individually for MC, NoMC and ICA1. Each voxel is given a value based upon how well the voxel time serie is described by the analysis model. A map with these values is called a goodness of fit map. The *difference in goodness* of fit is generated by subtracting one goodness of fit map from another, e.g., NoMC from MC and ICA1 from MC.

A positive value would indicate that MC is better at modelling data and a negative one would say NoMC (red curve) and ICA1 (green curve) is better.

The goodness of fit evaluation suggests that MC model better describes simulated data than NoMC. At low levels of motion (0.1 mm) the difference between the methods is insignificant but the difference between the two methods increases when motion size increases.

The goodness of fit evaluation for MC and ICA1 indicates that the two methods are equally successful in modelling data.

Goodness of fit for different correlation

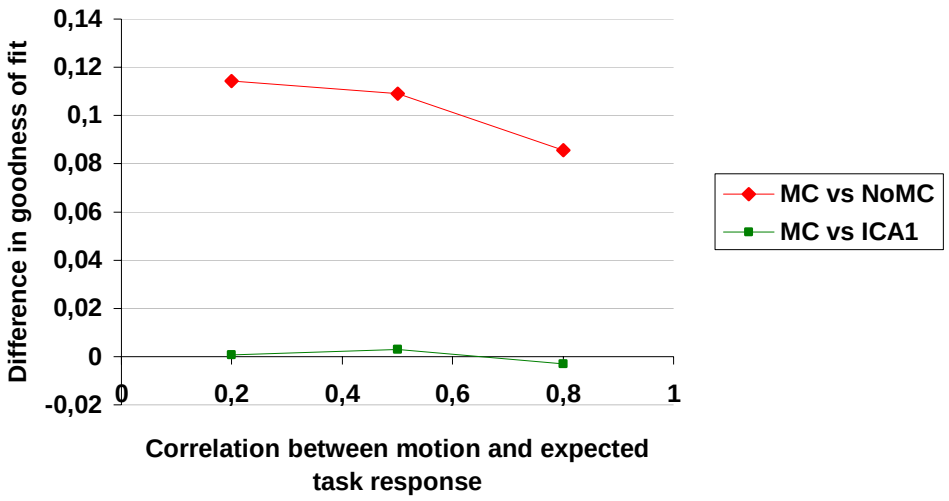

Figure 15. Difference in goodness of fit with motion size 1 mm. Positive value on the difference in goodness to fit-axis suggests that MC is more successful in describing the data while a negative would suggest NoMC or ICA1.

Figure 15 describes the goodness of fit as a function of correlation. A positive value would indicate that MC is better at identifying true activation and a negative one would mean that NoMC and ICA1 would be better.

The goodness of fit evaluation suggests the relative performances of the methods are independent of the correlation between motion and task response. Analysis with motion parameters as covariates is superior for all levels of correlations between task and motion. There is no major difference between MC and ICA1 when it comes to modelling the data with different correlations.

4.2 Patient data

4.2.1 t-ratio

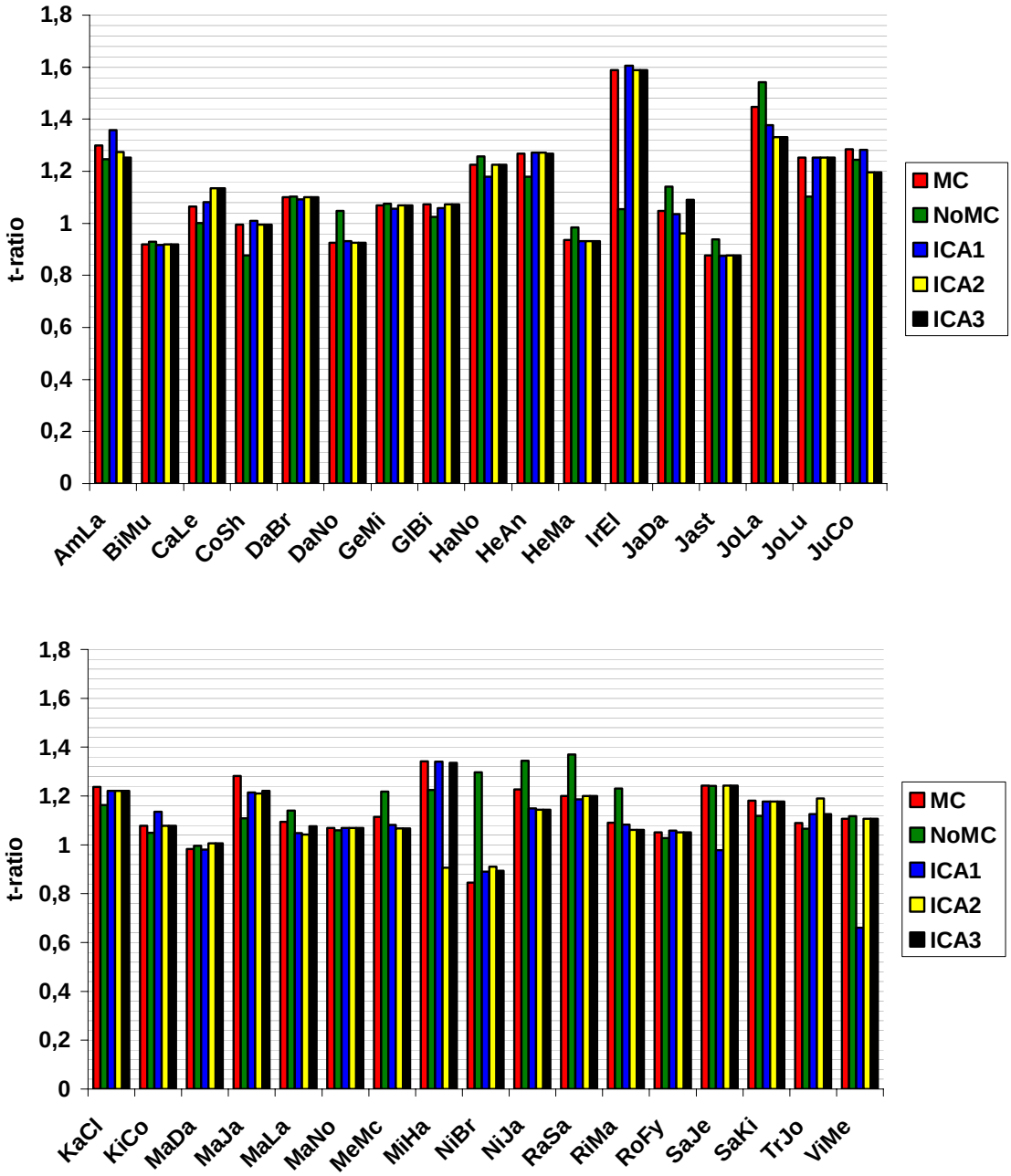

Figure 16. t-ratio, five different data sets for all 34 subjects. The subjects are sorted in an alphabetical order. A high t-ratio indicates a good performance.

In figure 16 we consider the t-ratio for every method and for each subject. A high t-ratio indicates that the method is successful in identifying activation inside our region of interest.

Results show that NoMC is the marginally superior method in 8 of the subjects and in one subject (NiBr) NoMC outperforms the other methods. MC performs marginally better in 7 of the subjects and outperforms NoMC in one subject (IrEl).

In 16 subjects there is no significant difference between the methods.

Only in a few subjects do MC and the ICA methods differ. One of the three ICA methods is superior for three subjects (AmLa, CaLe and TrJo), but ICA1 doesn't perform well for two subjects (SaJe and ViMe).

4.2.2 t-ratio as a function of subject motion

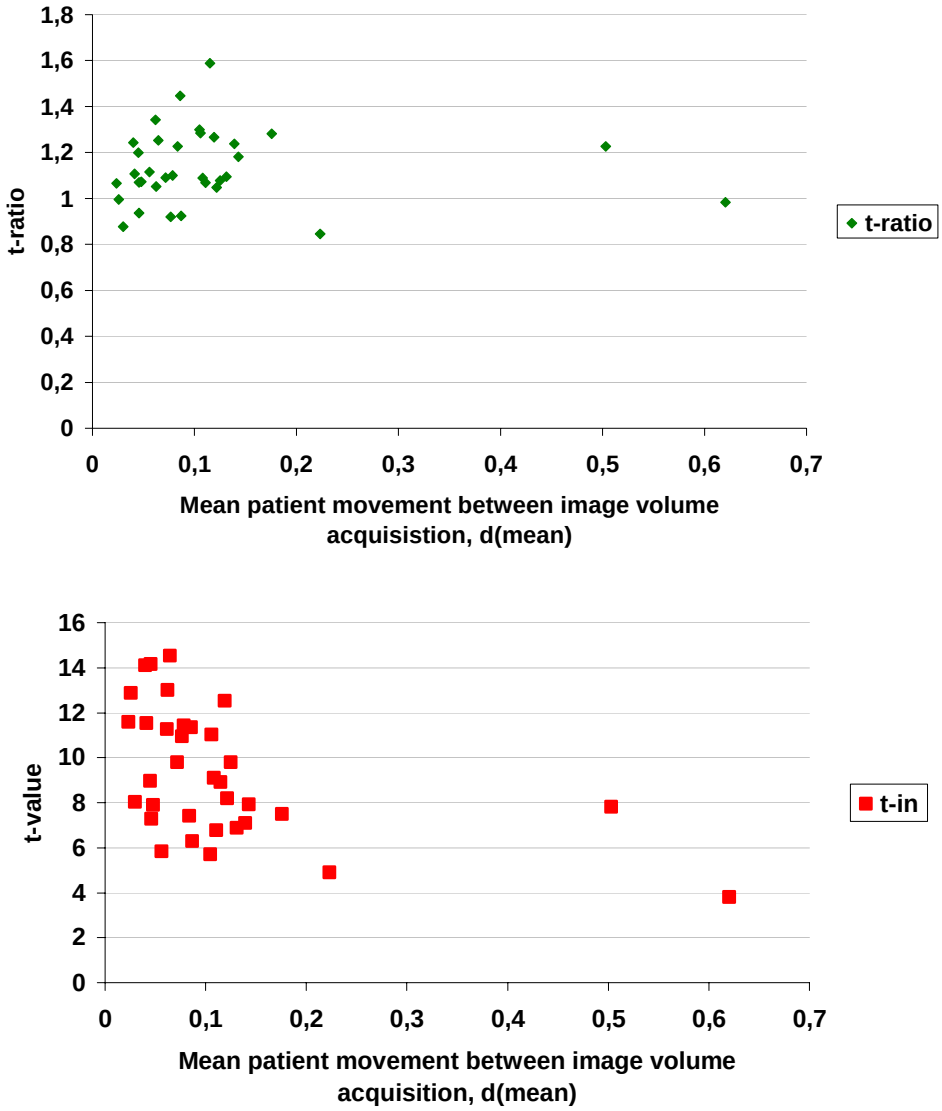

Figure 17. t-ratio (upper) and t_{in} (lower) as a function of mean motion between images for patient data. The t_{in} and t-ratio is plotted against the average translation between image volumes. d_{mean}-translation of 0.49 mm corresponds to 1 mm movement in simulated data. All subjects but two register an average movement lower than 0.3 mm which place them in the region below 1 mm in simulated data.

In figure 17 we consider the t-ratio (upper) and t_{in} (lower) as function of mean movement between image volumes in the estimated motion parameters for patient data. Each point represents the t-ratio or t-value for one subject after an analysis with motion covariates (MC).

The t-ratio is independent of mean motion size between images. t_{in} on the other hand decreases with an increase in mean motion and an unchanged ratio implies that t_{out} changes also decreases with higher mean motion.

The mean translation between images volumes for added simulated motion of 1 mm (fig. 6b upper graph) was 0.49 mm. All patients except two display lower d_{mean}. This fact places all our patients in the region below the corresponding simulated motion of 2 mm.

4.2.3 Goodness of fit

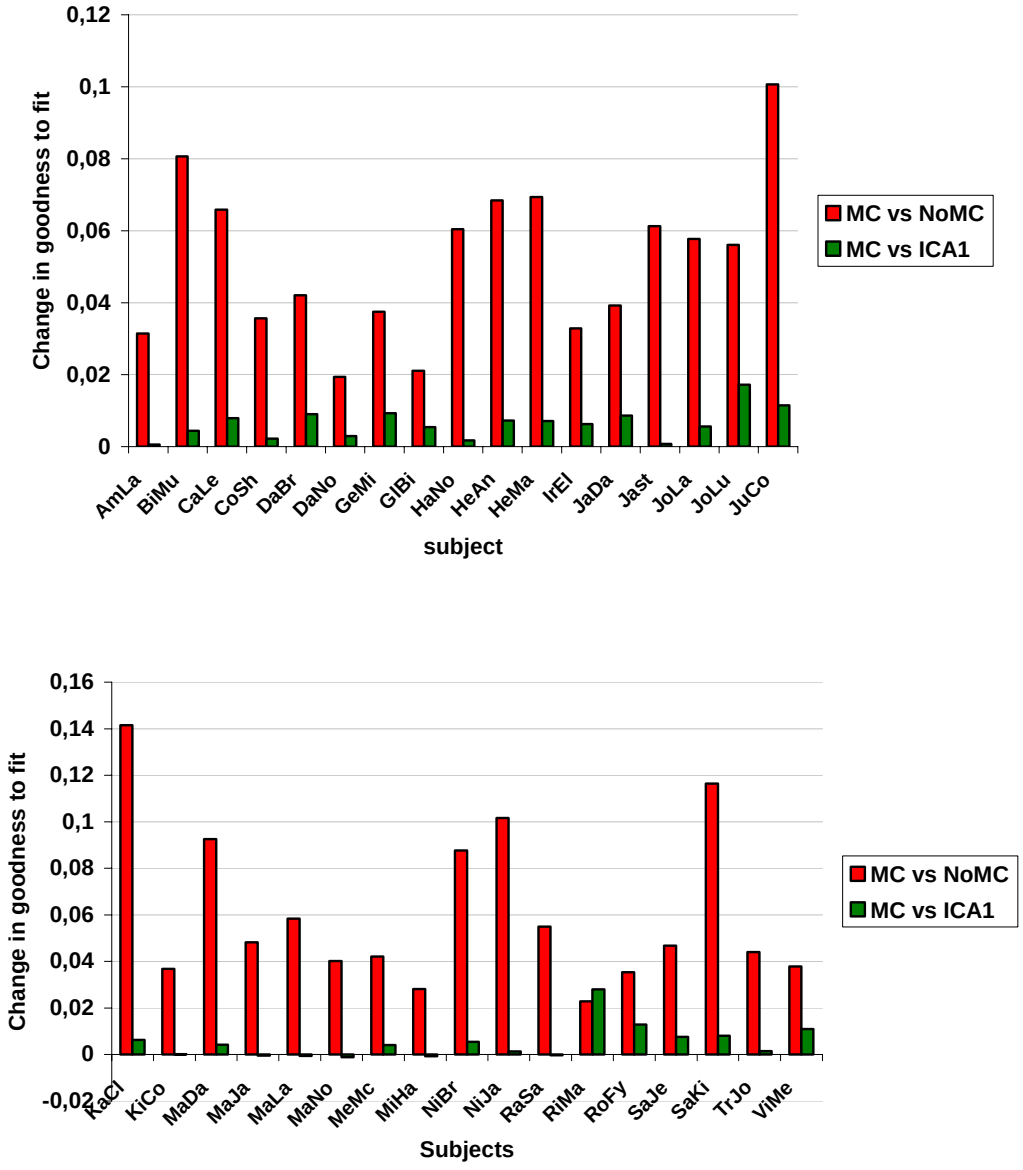

Figure 18. The mean value for goodness of fit for 34 subjects. The mean value of the delta images is displayed for each subject. The red bars for each subject describes which of MC and NoMC that best models the data. A positive value indicates that MC is best and a negative NoMC. The green bars are a comparison between MC (positive) and ICA (negative).

In figure 18 the difference in goodness to fit is displayed for all subjects. The red bars indicate which of the two methods MC and NoMC that is most successful in modelling the data. A positive value means that MC better models the data and a negative NoMC. The green bars show which of the two methods MC and ICA1 that best models the data. A positive difference in goodness of fit indicates that MC is better at modelling the data and a negative ICA1.

MC is more successful in modelling data for all subjects. A difference higher than 0.1 in goodness of fit between MC and NoMC is seen in four patients (JuCo, KaCl, NiJa, and SaKi).

MC and ICA show a similar performance although MC is better for all the subjects except for one (MaNo)

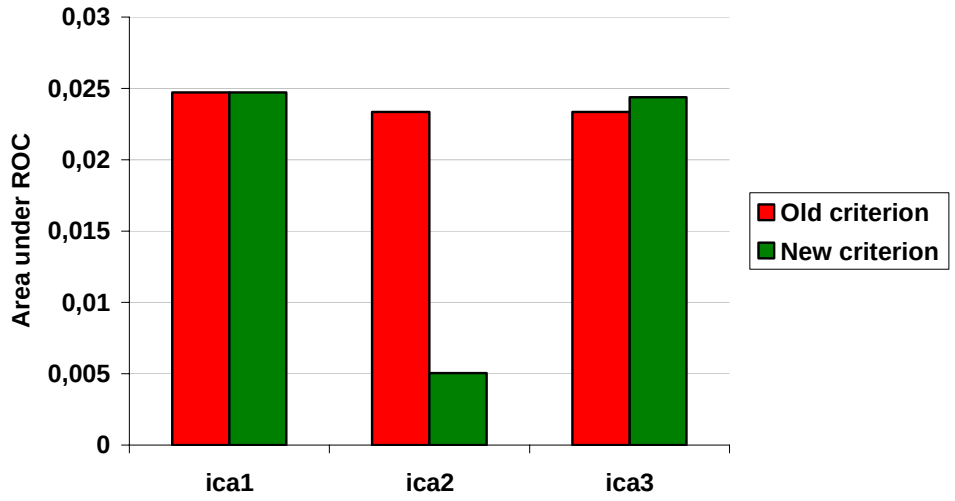

Figure 19. Comparison between two different ways to select components that contain motion induced variance. Red bars display the area under the curve for the old criterion and green for the new criterion. The two different criterions were tested on simulated data (correlation to motion = 0.5 and motion = 5mm).

Figure 19 displays the auROC for the three ICA methods. The old criterion was to select components with a high positive correlation to estimated motion parameters (red bars). But the true motion induced signal variance can also have a negative correlation. A better criterion would be to select the component based on the absolute value of the correlation to motion (green bars). There is hardly any difference between the two criterions in ICA1 and 3. The loss in performance with the new criterion for ICA2 is because one of the removed components was in fact true activation with high correlation to the motion parameters.

5. Discussion

Remove motion components with ICA

Our results from both simulated and patient data indicate that ICA can be successful in finding and removing motion induced signal changes, but not to the extent that it will greatly increase the specificity and sensitivity of the analysis.

These results contradicts previously performed studies were ICA have been successful in removing motion induced activation [13] and increasing the specificity and sensitivity of the analysis.

This conclusion is supported by both simulated data and patient data were one see no significant increase in performance after removal of supposed motion components. This specific method has not been suggested and evaluated previously so the choice of motion rejection thresholds was totally arbitrary. By fine tuning these thresholds one might better identify motion components and thus increase the specificity and sensitivity of the analysis.

ICA2 data had components with a correlation to the estimated motion parameters greater than 0.3 rejected. With a lower motion rejection threshold more components would be rejected. This could help increase the sensitivity of the analysis. But there is always a risk that the components with low correlation coefficient contain stimuli-induced variance. Especially if motion is well correlated to the expected BOLD response.

With ICA3 we identified components with a correlation to motion parameters greater than 0.3 and a correlation to expected task response lower than 0.3. These two thresholds could be altered in order to increase the sensitivity and specificity of the analysis.

One might argue that the analysis on data with removed motion components should be preformed without motion covariates. To investigate whether the use of motion covariates had any affect on analysis specificity and sensitivity, we performed an analysis on data sets with 5 mm motion and varying correlations. These results are seen in figure 10. Results do not differ from the analysis without covariates (NoMC) which suggest that the sensitivity and specificity of our analysis does not depend on whether we use covariates or not.

A limitation to our model is the criterion for selecting motion components, namely the component time series with high positive correlation to motion parameters. The true motion induced signal change can have a negative correlation coefficient. Therefore it would be better suited to select components by the absolute value of the correlation coefficient instead of the positive correlations.

The difference between the old and the new criterion for motion component removal is displayed in figure 19. The difference is not significant for method ICA1. One of the components removed in ICA2 with the new criterion is the stimuli-induced activation which decreases the auROC. Our third motion rejection method hinders this removal of true activation when it also takes in to account the individual component correlation to expected task response, but it does not produce a significantly greater result than with the old criterion.

The new criterion of removal of components must be further tested for simulated deta. It should also be applied to patient data before drawing any conclusions. We recommend that the components rejected are selected according to our new criterion; the absolute value of the correlation coefficient between motion parameters and expected response.

The use of motion parameters as covariates

AuROC evaluation on simulated data suggest a motion threshold (2 mm, see figure 10) were NoMC should be use if the subject motion is below the threshold and MC when motion

exceeds the motion threshold. NoMC demonstrate a higher number of true positive voxels when simulated motion is low relative to MC. This is because of stimuli induced signal variance being interpreted as motion induced variance and vice versa when motion parameters are added as covariates. Still, NoMC is the preferred analysis model according to simulated data.

All our patients' register a mean displacement between image volumes lower than the 2 mm threshold (image 17). If the conclusion drawn from simulated data is correct, NoMC analysis would be superior also for patient data.

According to our evaluation either NoMC or MC is more successful in analysing patient data. Instead they perform equally well. The use of t-ratio as evaluation method could be questioned. On the other hand t-ratio evaluation produces similar results to auROC when applied to identical data (fig 10 and 11).

The use of ROIs in patient data can also be a matter of discussion but we believe that the ROI is a good representation of the spatial location and distribution of the expected activation.

According to the difference in goodness of fit all data sets are best modelled by MC for both simulation and patient data. This is expected when one add more covariates to a model since more of the error variance can then be explained by the model. This effect is supposed to be compensated when we used the adjusted R^2, but the adjustment might not be able to entirely compensate for the adding of the new covariates. At the same time a better goodness to fit for one analysis model doesn't necessarily mean a better analysis performance; it is just an indication that MC better describes the data.

Both these observations devalue the credibility of difference in goodness of fit and the evaluation is most likely not a good measure of the analysis sensitivity or specificity.

Effects of task correlated motion

Results from both auROC and goodness to fit (simulated data) does not indicate that the choice of analysis model should be affected by the motion correlation to task. This is a contradiction to most of the literature on the subject today [2, 3, 4]. The results attained by A. Field et.al, shows that there are appreciable false activation artefacts even if motion is less than 1 mm. There are two possible ways to interpret the lack of motion induced activity; firstly that our evaluation methods are not sensitive enough to identify these artefacts and finally that there in fact is no extra spurious activation.

A visual examination of analysis results from un-realigned data sets with different correlation to stimuli displayed varying amounts of spurious activation. The amount of spurious activation was proportional to the correlation coefficient. This indicates that the second assumption is correct. So why is there no increase in spurious activation when correlation increases?

There is no major difference between analysis efficiency with or without motion parameters as effects of no interest. Is the added x-axis translation really complex enough? One argument could be that the realignment can successfully compensate for the movement and thus hinder spurious activation.

To test this argument we calculated the correlation coefficient between the added motion and the estimated motion. A correlation coefficient close to 1 would indicate that the realignment was perfect. The performance ranged from 0.79 to 0.92 which indicates that the realignment was not perfect and that there should be some residual motion that could influence the analysis.

We discovered an error in our simulated data in the late phase of our thesis. When an image volume was displaced to simulate large patient movement (~2 cm) some parts of the brain were moved outside the image volume. After realignment this displaced parts of the brain was missing. One would suspect that these artefacts would affect the accuracy in some parts of the pre-processing steps, particularly the realignment phase.

Further experimental trials on data sets with more complex motion design are needed. Another problem to address is the loss of data around the edges when simulated motion size is large. Considering these two aspects the current simulated data might not provide any valid conclusions. Our results contradict some of the most fundamental knowledge about correlated motion and its effects [2, 3, 4] and it is rather our simulated data and our methods that need to be question and reviewed than anything else.

Analysis dependence of signal amplitude

One would assume that the analysis performance would be proportional to the mean signal strength. Instead this assumption is contradicted by the auROC-evaluation (fig. 13). It shows an increase in analysis performance for all data sets between 1 and 2%. But between 2 and 5% there is just a small increase in analysis sensitivity and specificity.

The reason for this is unclear but we suspect that our analysis successfully identifies nearly all voxels containing added activation. When the signal strength increases there is no visible increase in analysis efficiency because there is just a limited amount of true positive voxels left to identify.

6. Conclusions

Remove motion components with ICA

With our current criterion for selecting motion components we fail to localize and remove motion induced artefacts to a satisfying extent. We have suggested a new criterion for selection of motion component which is likely to be more sensitive in detecting motion induced variance.

The use of motion parameters as covariates

The reliable auROC evaluation identifies NoMC as the most successful method for identifying true activation when motion is lower than 2 mm. This is contradicted by our patient data were no method is superior even though all patient displays movement less than 2 mm.

Effects of task correlated motion

In this study we did not se any evidence of an increase or decrease in motion induced activation when the correlation between added motion and task was altered. This contradicts the conclusions in a number of studies [2, 3, 4].

A method that assures that no vital data is lost when adding high motion to data sets must be developed before one can argue about the validity of these results.

Analysis dependence of signal amplitude

Our analysis is successful at identifying most of the true positives and almost no false positives at 2%, i.e close to finding the ground truth. A further increase in signal strength will only slightly increase the analysis performance.

7. Acknowledgement

I would like to thank my friend and supervisor Tony Waites for his commitment to my thesis and the fact that he invited me to his home in the early parts of our stay.

I would also like to thank our co-supervisor Freddy Ståhlberg and our Director of Graduate Students Bo-Anders Jönsson who assisted me in the preparation for this journey.

I would like to thank everyone at Brain Research Institute for always being helpful and friendly. Special thanks go out to Gaby Pell and Richard Masterton for all their help. Without their patience and endurance this thesis would not have been possible.

Finally I would like to thank Emil Johansson, who is a great friend and fellow student, for all the help during the thesis and for the good times we have had together during our time down under.

8. References

[1] T Krings, M H T Reinges, S Erberich, S Kemeny et.al. **Functional MRI for presurgical planning: problems, artefacts, and solution strategies.** J. Neurol. Neurosurg. Psychiatry 2001; vol 70;749-760

[2] K J Friston, S Williams, R Howard, R S J Frackowiak et.al. **Movement-related effects in fMRI time-series.** Magn Reson Med 1996; vol 35:346–355

[3] A S Field, Y Yen, J H Burdette, A D Elster. **False Cerebral Activation on BOLD Functional MR Images: Study of Low-amplitude Motion Weakly Correlated to Stimulus.** Elster AJNR Am J Neuroradiol 2000; vol 21:1388–1396, September

[4] J V Hajnal, R Myers, A Oatridge, J E Schwieso et.al. **Artifacts due to stimulus correlated motion in functional imaging of the brain**. Magn Reson Med 1994; vol 31:283–291

[5] T Johnstone, K S Ores Walsh, L L Greischar et.al. **Motion Correction and the Use of Motion Covariates in Multiple-Subject fMRI Analysis.** Human Brain Mapping 2006; vol 27:779 –788

[6] R S J Frackowiak, K J Friston et.al. **Human Brain Function**. Academic Press 1997

[7] P Jezzard, P M Matthews, S M Smith. **Functional MRI; an introduction to methods**. Oxford University Press 2001.

[8] V Edward, C Windischberger, R Cunnington et.al. **Quantification of fMRI Artifact Reduction by a Novel Plaster Cast Head Holder**. Human Brain Mapping 2000; vol 11:207–213

[9] S Thesen, O Heid, E Mueller, L R Schad. **Prospective acquisition correction for head motion with image-based tracking for real-time fMRI.** Magn Reson Med 2000; vol 44(3);457-65.

[10] L Freire, A Roche, J F Mangin. **What is the best similarity measure for motion correction in fMRI time series?** IEEE Trans Med Imaging 2002 May; vol 21(5):470-84

[11] F Ezposito, E Formisano, E Seifritz, R Goebel. **Spatial Independent Component Analysis of Functional MRI Time-Series: To What Extent Do Results Depend on the Algorithm Used**. Human Brain Mapping 2002; vol 16:146-157

[12] V. D. Calhoun et al. Web: http://icatb.sourceforge.net/

[13] T Kochiyama, T Morita, T Okada, Y Yonekura et.al. **Removing the effects of task-related motion using independent-component analysis**. NeuroImage 2005; vol 25:802-814

[14] P Skudlarski, R T Constable, and J C Gore**. ROC Analysis of Statistical Methods Used in Functional MRI:Individual Subjects**. NeuroImage 1999; vol 9:311–329

[15] R T Constable, P Skudlarski, E Mencl, K R Pugh. **Quatifying and comparing region-of-interest activation patterns in functional brain MR Imaging: Metholodgy**. Magn Res Imag 1998; Vol. 16; 3:289–300

[16] T Huu Le and X Huw. **Methods for Assessing Accuracy and Reliability in Functional MRI**. 1997; vol 10:160–164

[17] A B Waites, P Mannfolk, M E Shaw, J Olsrud. **Flexible statistical modelling detects clinical functional magnetic resonance imaging activation in partially compliant subjects**. 2007

[18] A B Waites, R S Briellmann, M M Saling, D F Abbott et.al. **Functional Connectivity Networks Are Disrupted in Left Temporal Lobe Epilepsy.** Ann Neurol 2006;59:335–343

[19] O Speck, J Hennig, M Zaitsev. **Prospective Real-time Slice-by-slice motion correction for fMRI in Freely Moving Subjects**. MAGMA 2006; e-publicised ahead of print.

[20] http://www.fil.ion.ucl.ac.uk/spm/doc/books/hbf2/pdfs/Ch7.pdf
J Ashburner, K Friston, W Penny, S J Kiebel, A P Holmes. **The general linear model.** Human Brain function, Second edition.